Heat Conduction in $Ba_{1-x}K_xBiO_3$

Ctirad Uher,[1] Frank Tsui,[1] Baoxing Chen,[1] and P. D. Han[2]

We have investigated heat conduction of single crystal $Ba_{1-x}K_xBiO_3$ in the temperature range of 2 - 300 K and in a magnetic field of up to 6 Tesla. Temperature dependence of thermal conductivity $\kappa(T)$ reveals the participation of both electrons and phonons with their relative contributions that depend critically on the potassium doping concentration. Crystals underdoped with potassium (samples with higher T_c) exhibit a strong suppression of κ and a glass-like temperature dependence. In contrast, those with a higher potassium content (lower T_c) show an increase as temperature decreases with a peak near 23 K. Field dependence of $\kappa(H)$ is also very sensitive to the level of potassium doping. Crystals exhibiting a large phonon contribution show an initial drop in $\kappa(H)$ at low fields followed by a minimum and then a slow rise to saturation as the field increases. The initial drop is due to the additional phonon scattering by magnetic vortices as the sample enters a mixed state. The high field behavior of $\kappa(H)$, arising from a continuous break-up of Cooper pairs, exhibits scaling which suggests the presence of an unconventional superconducting gap structure in this material.

1. INTRODUCTION

The discovery of superconductivity in $Ba_{1-x}K_xBiO_3$ (BKBO) [1,2] and its unique physical properties have stimulated considerable interest. Unlike the copper-oxide layered perovskite superconductors, BKBO is cubic and copperless, contains no magnetic ions, and exhibits a large isotope effect [3]. These and other features suggest that electron-phonon coupling is the relevant mechanism for superconductivity in this compound. Owing to its moderately long coherence length, low microwave loss, and good tunneling characteristics, BKBO is also attracting interest for technological superconductor applications.

One of the less fortunate aspects of BKBO is the presence of mixed phases and a tendency for an inhomogeneous distribution of potassium [4], both of which contribute to a rather high electrical resistivity. This results in considerable difficulties when attempting to determine the essential galvanomagnetic transport parameters. Thermal transport, on the other hand, avoids these problems, and it probes directly the behavior of carriers and phonons in both the normal and the supercon-

ducting states [5,6]. A few years back we have reported on the thermopower and thermal conductivity of polycrystalline BKBO [7]. In this paper we report on our recent studies made on high quality single crystals. We show that the thermal conductivity is rather sensitive to the potassium doping concentration, and we provide first results on the magnetic field dependent heat conduction of BKBO crystals.

2. EXPERIMENTAL

Measurements were made on single crystals prepared by a three-electrode, top-seeded growth method [8]. This method facilitates the growth of relatively large crystals with T_c of up to 32 K and sharp superconducting transitions. It provides a possibility to control potassium content by imposing an overpotential. The samples used in this study were typically 1 to 2 mm long and about 1 mm across. We describe results on two samples: sample A with T_c = 18 K, and sample B with a lower potassium content (underdoped) and T_c = 30 K.

Magnetization measurements were carried out using a commercial SQUID magnetometer in order to determine the T_c, the width of the transition, and the magnetic irreversibility. We focused our measurements on two types of sweeps: zero-field-cooled (ZFC) and field-cooled (FC) sweeps at a fixed field (Fig. 1a), and field dependent

[1]Department of Physics, University of Michigan, Ann Arbor, Michigan 48109-1120.
[2]Department of Materials Science and Engineering, University of Illinois at Urbana-Champaign, Urbana, Illinois 61801.
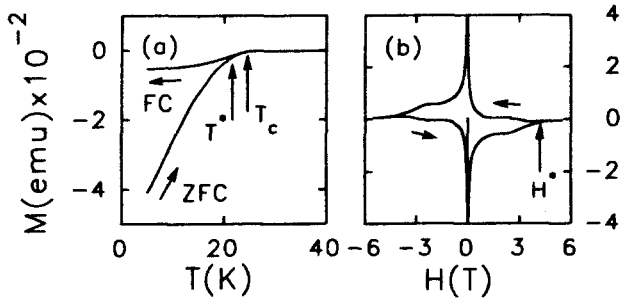
Fig. 1. Typical magnetic hysteresis loops for sample B. (a) Temperature dependent hysteresis curve between zero-field-cooled (ZFC) and field-cooled (FC) magnetizations at 3 Tesla. Arrows indicate T^* and T_c, respectively. (b) Field dependent hysteresis at 20 K. The irreversibility field H^* is indicated by the arrow.

hysteresis at a fixed temperature (Fig. 1b). The irreversibility field H^* and temperature T^* are determined from the points of divergence in the hysteretic traces, as indicated in Fig. 1.

Thermal conductivity was measured by a steady-state technique with the aid of a miniature resistive heater and two pairs of differential chromel-constantan thermocouples. The thermocouples were calibrated to account for small changes in their electromotive force in a magnetic field. Fields of up to 6 Tesla were supplied by a superconducting split-coil magnet, and were directed perpendicular to the heat current.

3. RESULTS

3.1. Magnetization

Our magnetization measurements were designed to probe flux pinning behavior by investigating the magnetic irreversibility and the associated critical parameters, H^* and T^*. The temperature dependent magnetization exhibits Meissner effect below T_c, as shown in Fig. 1a. The irreversibility temperature T^* coincides with T_c at zero field, and it decreases as field increases; the irreversibility field H^*, on the other hand, increases correspondingly with decreasing temperature. Below T_c, the measured H^* is much smaller than the upper critical field H_{c2} (see Fig. 1b). The width of the magnetic hysteresis loop (e.g. Fig. 1), to a good approximation, is directly proportional to the critical current [9].

Fig. 2 traces the irreversibility of sample B. The observed behavior exhibits scaling in the form

$$H^* \sim (1 - T^*/T_c)^3. \tag{1}$$

The exponent of 3 has been observed in $Ba_2Sr_2CaCu_2O_8$ [10], but not in sample A nor other BKBO [11,12] nor in

$YBa_2Cu_3O_7$ [10], where an exponent of 3/2 is reported. It has been shown [10,13] that the flux pinning energy and its temperature and field dependences determine the scaling exponent. When flux lines are rigid corresponding to a large pinning energy and collective pinning effects, an exponent of 3 is expected; when flux bundles are weakly correlated, one expects a smaller pinning energy and an exponent of 3/2. The observed exponent for sample B reveals the presence of a high defect concentration arising from potassium underdoping, which leads to stronger pinning effects. More insights on the effects of potassium doping, particularly its influence on the superconducting transition, are obtained from thermal conductivity measurements described below.

3.2. Thermal Conductivity

The temperature dependences of $\kappa(T)$ for samples A and B are shown in Fig. 3. They represent various scattering processes that involve different length scales in these samples. The underdoped sample B exhibits a strong suppression of thermal conductivity compared with sample A, more than a factor of 10 at low temperatures. This is attributed to a reduction in phonon mean free path in underdoped samples due to defects. The estimated phonon mean free path for sample B at 25 K is about 10 Å using data from specific heat measurements [14], and it is expected to be even shorter at higher temperatures. This length scale corresponds to a defect density of nearly one per unit cell. The apparent high defect density may arise from statistical fluctuations of dopant concentration from one unit cell to another in underdoped samples. The high temperature behavior of sample B exhibits a slow increase with temperature (Fig. 3) similar to that of the polycrystalline samples [7]. The behavior is consistent with the short mean free path, and thus a glass-like temperature dependence [15]. It is not that unusual to see glassy behavior in crystalline
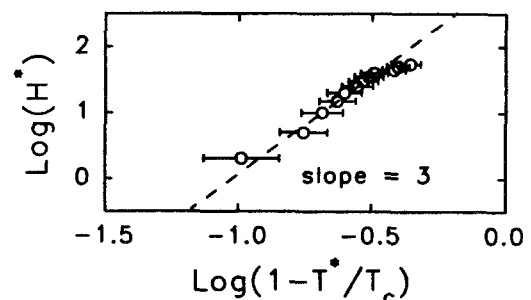

Fig. 2. Log-log plot of irreversibility field H^* versus the reduced irreversibility temperature $(1 - T^*/T_c)$ for sample B. $T_c = 30$ K.

materials; other examples do exist [16,17]. The behavior for sample A, on the other hand, exhibits a decrease as temperature increases which indicates a strong phonon conductivity dominated by Umklapp processes [15]. This is consistent with a low defect density and the crystalline nature of the sample.

As temperature decreases, the rise in heat conduction of sample A slows down; then it rises to a distinct peak around 23 K, before it drops at lower temperatures. Sample B exhibits no such peak, but it also displays a similar decrease at low temperatures. The peak observed in sample A evidently arises from the transition between the high temperature phonon dominated conduction and the low temperature drop due to phonon scattering by imperfections [15]. We believe that the peak is not directly related to the onset of superconductivity, because it occurs well above T_c. As mentioned above, the grain boundaries and scattering centers in these samples arise from the inevitable statistical fluctuations of K doping concentration. We have ruled out the participation of the electronic thermal conduction at this temperature because most electrons are condensed into Cooper pairs. It is also unlikely that a strong suppression of quasiparticle scattering [18] plays any role here, according to the field dependent results discussed below.

More evidence on a large phonon thermal conductivity of sample A is obtained from the field dependent behavior shown in Fig. 4a. For increasing field, κ drops initially at low field and, after reaching a 'dip' at H_d, it slowly rises to saturation. The initial rise in $1/\kappa$ (Fig. 4a, inset) is due to additional phonon scattering by magnetic vortices as the sample enters a mixed state. It cannot be attributed to electron scattering by vortices because the electron mean free path is less than 10 Å, as indicated by results from our measurements and those of others [3,12]. For a 'dilute' system of vortices, the additional phonon scattering is approximately laH/Φ_0 [19] with l the phonon mean free path, a the diameter of the vortex line, Φ_0 the flux quantum, and H the magnetic field. The phonon thermal resistivity $1/\kappa_{ph}(H)$ in this limit is, therefore, linear with H.

The linear dependence fits the observation rather well (see inset in Fig. 4a) with a slope that depends on the product of l and a. At higher fields the strong interaction between vortices leads to the formation of a flux lattice, and consequently phonon scattering by vortices diminishes; thus κ_{ph} no longer drops at H_d. This happens when the penetration depth λ is comparable to the separation of flux lines, so while λ increases with increasing temperature H_d decreases.

The slow rise of κ above H_d arises from increasing electronic contribution due to the continuous break-up of Cooper pairs. This enables us to estimate the electronic contribution κ_e from the size of the total increase in $\kappa(H)$. For instance, at 4.6 K, κ_e is less than 1/5 of the
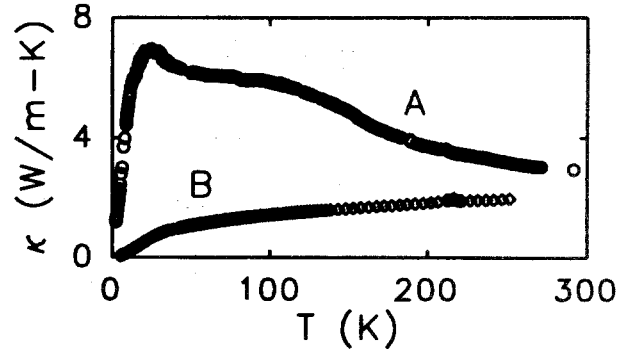

Fig. 3. Temperature dependence of the thermal conductivity for sample A (open circles) and sample B (open diamonds).

total κ in the normal state. From this we estimate the phonon contribution and the phonon mean free path l using the published specific heat data [14]; at 4.6 K l is ~ 4000 Å. The large mean free path makes the initial drop in $\kappa(H)$ possible because, if l is shorter than the average distance between vortices, κ_{ph} would not be affected by them. Note that the vortex spacing of 4000 Å corresponds to a field strength of about 100 G. The observed large drop at low fields further supports the notion that the phonon contribution dominates the zero field heat conduction.

In sample B the higher defect concentration leads to a shorter phonon mean free path (~ 100 Å at 4.6 K), hence a smaller phonon contribution to the thermal conductivity. This in turn results in a smaller or no phonon dip in $\kappa(H)$ at low fields. Although the electronic thermal conductivity of sample B is actually comparable to that of sample A, the observed large rise in $\kappa(H)$ for sample B at high fields indicates that its electronic part represents a greater fraction of the conductivity than that in sample A.
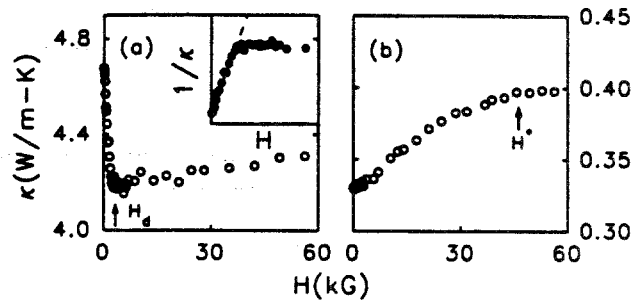

Fig. 4. Field dependent thermal conductivity (a) for sample A at 9.2 K and (b) for sample B at 15.2 K. Inset of (a) shows the corresponding thermal resistivity which exhibits linear behavior at low fields (dashed line). Arrows indicate H_d in (a) and H^* in (b). Note that the two temperatures in (a) and (b) correspond roughly to the same T/T_c value (~ 0.5).

At higher fields, the measured thermal conductivity saturates at a critical field H^*, which is far below H_{c2} (> 5.5 Tesla just below $0.8T_c$, see Section 3.1) obtained from magnetization measurements. The behavior below H^* exhibits scaling in the form

$$\kappa(H^*) - \kappa(H) \sim (H^* - H)^{3/2}, \qquad (2)$$

as shown in Fig. 5 for sample B. Eq. (2) corresponds approximately to the electronic thermal conductivity in the superconducting state, κ_{es}. The 3/2-power law differs from the linear behavior of the conventional dirty type-II superconductors [20] given by

$$\kappa(H_{c2}) - \kappa(H) \sim (H_{c2} - H). \qquad (3)$$

The observed functional dependence on field suggests the presence of an unusual gap structure in BKBO. In a separate publication [21] we derive self consistently the effective gap from the observed field dependence [Eq. (2)] using a BCS-like treatment [22]. The resulting effective gap in BKBO is given by [21]

$$\varepsilon(H) \sim (H^* - H)^{1/2}, \qquad (4)$$

with H^* the field at which the effective gap vanishes. The measured H^* coincides with magnetic irreversibility field obtained from magnetization measurements (Section 3.1). The latter field signals the onset of supercurrent. It is reasonable to conclude that both fields are the same, and that they also determine the onset of the unconventional superconducting gap given by Eq. (4).

The mean-field-like superconducting gap, indicated by the exponent of 1/2 [Eq. (4)], appears to exist in all BKBO crystals we have studied. However, its effects on thermal conductivity are more pronounced in potassium underdoped samples with higher T_c, because the phonon contribution is suppressed by the higher defect concentration, as discussed above. The presence of a robust gap

with a relatively high critical field H^* suggests that the electron-phonon interactions in BKBO are quite strong. While potassium concentration affects directly the thermal conductivity of BKBO through phonon mean free path, it does not appear to influence the form and strength of the gap.

4. CONCLUSION

We have studied the magnetic irreversibility and thermal conductivity of BKBO crystals in a wide range of temperatures and fields. The different roles of electrons and phonons on thermal conduction are examined. Our results reveal that both thermal conductivity and superconducting transition can be tuned by potassium doping concentration, and that the statistical fluctuation of the K concentration determines the phonon mean free path and the character of flux pinning. The observed scaling behavior for the high field thermal conductivity indicates the presence of an unconventional and mean-field-like gap structure in BKBO. The gap and the related phenomena reveal insight into the fundamental processes that cause the superconductivity in BKBO.

ACKNOWLEDGMENTS

REFERENCES

1. L. F. Mattheiss, E. M. Gyorgy and D. W. Johnson, *Phys. Rev. B* **37**, 3745 (1988).
2. R. J. Cava, *et al.*, *Nature* **332**, 814 (1988).
3. B. Batlogg, *et al.*, *Phys. Rev. Lett.* **61**, 1670 (1988).
4. E. S. Hellman and E. H. Hartford, *Phys. Rev. B* **47**, 11346 (1993).
5. C. Uher, *J. Supercond.* **3**, 337 (1990).
6. C. Uher, in *Physical Properties of High Temperature Superconductors III*, edited by D. M. Ginsberg, (World Scientific, Singapore, 1992), p. 159.
7. S. D. Peacor, *et al.*, Phys. Rev. B **42**, 2684 (1990).
8. P. D. Han, L. Chang and D. A. Payne, *J. Crystal Growth* **128**, 798 (1993).
9. C. P. Bean, *Phys. Rev. Lett.* **8**, 250 (1962); *Rev. Mod. Phys.* **36**, 31 (1964).
10. C. C. Almasan, *et al.*, *Phys. Rev. Lett.* **69**, 3812 (1992).
11. Y. Y. Xue, *et al.*, *Physica C* **194**, 194 (1992).
12. B. Chen, F. Tsui and C. Uher, unpublished.
13. J. C. Garland, C. C. Almasan, and M B. Maple, *Physica C* **191**, 158 (1992).
14. G. K. Panova, *et al.*, *JETP* **76**, 302 (1993).
15. R. Berman, *Thermal Conduction in Solids*, (Clarendon Press, Oxford, 1976).
16. P. B. Allen, *et al.*, *Phys. Rev. B* **49**, 9073 (1994).
17. D. G. Cahill and R. O. Pohl, *Phys. Rev. B* **35**, 4067 (1987).
18. R. C. Yu, *et al.*, *Phys. Rev. Lett.* **69**, 1431 (1992).
19. J. Lowell and J. B. Sousa, *J. Low Temp. Phys.* **3**, 65 (1970).
20. D. Saint-James, G. Sarma and E. J. Thomas, *Type II Superconductivity*, (Pergamon Press, Oxford, 1969).
21. B. Chen, *et al.*, *Phys. Rev. B*, submitted.
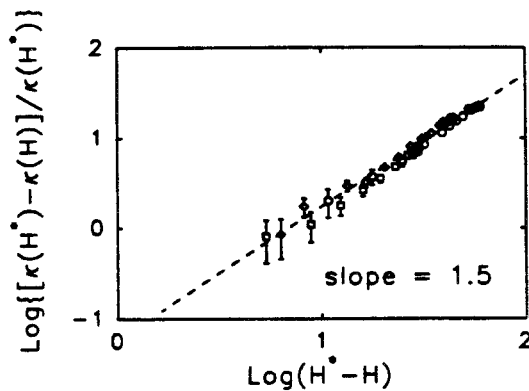22. J. Bardeen, G. Rickayzen and T. L. Tewordt, *Phys. Rev.* **113**, 982 (1959).

Fig. 5. Scaling behavior of thermal conductivity of sample B at three different temperatures: 12.4 K (circles), 15.2 K (diamonds), and 19.8 K (squares). The respective H^* for the three temperatures are 3, 4.5, and 6 Tesla. The dashed line corresponds to a slope of 1.5.